Functional and Structural Changes in a Canine Model of Hereditary Primary Angle-Closure Glaucoma

Sinisa D. Grozdanic,[1] *Helga Kecova,*[1] *Matthew M. Harper,*[1] *Wijitha Nilaweera,*[1] *Markus H. Kuehn,*[2] *and Randy H. Kardon*[2,3]

Purpose. To characterize functional and structural changes in a canine model of hereditary primary angle-closure glaucoma.

Methods. Intraocular pressure (IOP) was evaluated with tonometry in a colony of glaucomatous dogs at 8, 15, 18, 20, and 30 months of age. Retinal function was evaluated using electroretinography (scotopic, photopic, and pattern). Examination of anterior segment structures was performed using gonioscopy and high-frequency ultrasonography (HFU).

Results. A gradual rise in IOP was observed with an increase in age: 8 months, 14 mm Hg (median value); 15 months, 15.5 mm Hg; 18 months, 17.5 mm Hg; 20 months, 24 mm Hg; 30 months, 36 mm Hg. Provocative testing with mydriatic agents (tropicamide and atropine 1%) caused significant increases in IOP (35% and 50%, respectively). HFU analysis showed complete collapse of iridocorneal angles by 20 months of age. Scotopic and photopic ERG analysis did not reveal significant deficits, but pattern ERG analysis showed significantly reduced amplitudes in glaucomatous dogs (glaucoma, 3.5 $\pm$ 0.4 μV; control, 6.2 $\pm$ 0.3 μV; $P = 0.004$; Student's *t*-test). Histologic analysis revealed collapse of the iridocorneal angle, posterior bowing of the lamina cribrosa, swelling and loss of large retinal ganglion cells, increased glial reactivity, and increased thickening of the lamina cribrosa.

Conclusions. Canine hereditary angle-closure glaucoma is characterized by a progressive increase in intraocular pressure, loss of optic nerve function, and retinal ganglion cell loss. (*Invest Ophthalmol Vis Sci.* 2010;51:255–263) DOI:10.1167/iovs.09-4081

Glaucoma is characterized as a progressive optic neuropathy with characteristic optic disc changes and progressive visual field deficits.[1] Elevated intraocular pressure (IOP) is considered a primary risk factor for the initiation and progression of glaucomatous neuropathy.[1,2] However, in many patients, despite adequate control of the IOP, the loss of vision continues to progress, which necessitates further identification of molecular mechanisms responsible for the glaucomatous neurodegeneration and development of novel therapeutic modalities that directly target disease-affected retinal ganglion cells (RGCs).[2–4] Despite new discoveries, the underlying genetic abnormalities and environmental factors that may contribute to the development and progression of glaucoma have not been clearly defined.[5,6] Glaucoma in humans is typically a chronic and slowly progressive disease that may cause significant damage to the optic nerve before any symptoms of the disease are recognized. The gradual and often silent progression of the disease creates difficulties in early diagnosis and understanding of early changes in glaucomatous eyes. To better understand early glaucomatous changes and to develop effective diagnostic and therapeutic modalities, it is essential to create animal models that recapitulate the silent and slow development of the disease characterized by a progressive loss of RGC function.

Numerous inducible animal models of glaucoma have been used successfully to test different therapeutic strategies and to evaluate molecular mechanisms of RGC damage resulting from chronic elevation of IOP.[2,7,8] However, the major obstacles in many of these models is a very high elevation of IOP immediately after glaucoma induction surgery,[9–11] the inability to sustain elevated IOP longer than a period of a several months,[12–17] and the size of the eye, which is dramatically smaller than the human eye, posing a problem for effective translation of therapeutic options to the human patients.[18,19] Spontaneously occurring animal models of glaucoma in mice and dogs have also been described and have provided important information about the structural and molecular events occurring during the development of glaucomatous optic neuropathy.[20–26] Spontaneously occurring large animal models of glaucoma offer a unique opportunity to collect data by using instrumentation identical to that used in human patients with glaucoma. They are an excellent tool for the rapid development and translation of novel medical and surgical therapies from animals to human patients, and they provide interesting data correlating morphologic or biochemical findings to functional parameters.

The principal purpose of this manuscript was to describe the morphologic and functional changes in a canine model of hereditary primary angle-closure glaucoma (PACG). We hope this model will further advance our understanding of early functional, structural, and molecular changes in glaucomatous eyes.

Methods

All animal studies were conducted in accordance with the ARVO Statement for Use of Animals in Ophthalmic and Vision Research, and procedures were approved by the Iowa State University Committee on

From the [1]Department of Veterinary Clinical Sciences, College of Veterinary Medicine, Iowa State University, Ames, Iowa; [2]Department of Ophthalmology and Visual Sciences, University of Iowa Hospitals and Clinics, Iowa City, Iowa; and [3]Veterans Administration Medical Center, Iowa City, Iowa.

Supported by Department of Veterans Affairs, Veterans Health Administration, Rehabilitation Research and Development Service Grant C3919R; Iowa State University Biotechnology Fund; Fight for Sight; and an unrestricted grant from Research to Prevent Blindness.

Submitted for publication June 3, 2009; revised July 15 and 23, 2009; accepted July 24, 2009.

Disclosure: **S.D. Grozdanic**, None; **H. Kecova**, None; **M.M. Harper**, None; **W. Nilaweera**, None; **M.H. Kuehn**, None; **R.H. Kardon**, None

Corresponding author: Sinisa D. Grozdanic, Department of Veterinary Clinical Sciences, College of Veterinary Medicine, Iowa State University, Ames, IA 50011; sgrozdan@iastate.edu.

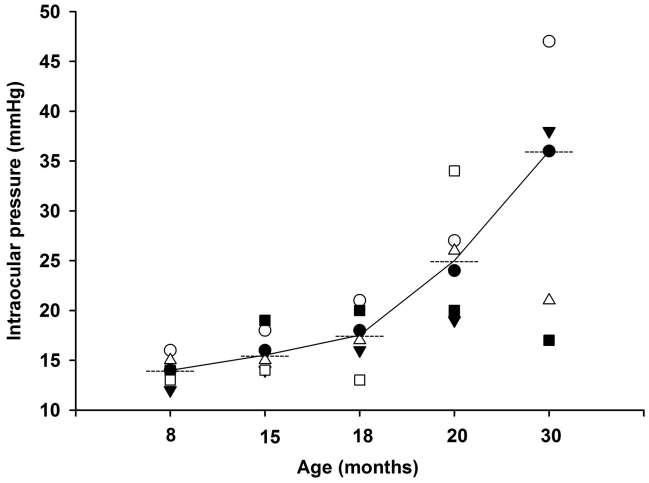

FIGURE 1. Development of elevated IOP in our colony of Basset Hounds. IOP increased progressively and significantly with advancing age. *Horizontal lines*: median values. Each symbol represents one animal ($n = 6$). Thirty-months time point has data from only five animals because both eyes of one animal were collected between 20 and 30 months of age.

Animal Care. Eight Basset Hounds from our colony (sire and dam affected with primary glaucoma, six of their offspring [F1 generation], and two dogs of F2 generation) were used for the evaluation of functional, structural, and IOP changes. Three additional dogs with PACG (two Siberian Husky dogs and one Shetland Sheepdog) were used for pattern ERG analysis. Additionally, 17 adult healthy Beagles and 12 young Beagles (6–8 months of age) were used as control animals. All control animals underwent ocular examination (slit lamp biomicroscopy, intraocular pressure evaluation, indirect ophthalmoscopy, gonioscopy, streak retinoscopy) to rule out the possible presence of ocular disease before inclusion in the study.

Intraocular Pressure Monitoring

Intraocular pressure was measured with a hand-held tonometer (TonoPen XL; Mentor, Norwell, MA) after application of topical anesthetic on the corneal surface (0.5% proparacaine hydrochloride; Falcon Pharmaceuticals, Fort Worth, TX) in awake animals for calculation of IOP data presented in the Figure 1, whereas IOP measurements used for the calculation of IOP versus pattern ERG regression analysis (see Fig. 6B) were taken 1 minute before the start of pERG recordings in anesthetized animals. All animals were extensively socialized; therefore, routine ocular examination could be performed with minimal to no restraint.

Electroretinography

Electroretinography was used to evaluate retinal function in control and glaucomatous dogs. Dogs were anesthetized with halothane 2.5% and a mixture of nitrous oxide and oxygen (30:70 ratio), body temperature was maintained using a heating pad, and systolic blood pressure was evaluated with an ultrasonic Doppler flow detector (Model 811-L; Parks Medical Electronics, Inc., Aloha, OR) every 5 minutes, immediately before and during pERG recordings. Neuromuscular paralysis was achieved using intravenous atracurium besylate (0.2 mg/kg body weight; Bedford Laboratories, Bedford, OH), and mechanical positive pressure ventilation was established to provide respiratory support and maintain oxygen saturation above 95%. The pupils were dilated with topical 10% phenylephrine hydrochloride (Ak-dilate; Akorn Inc., Buffalo Grove, IL) and 1% tropicamide (Tropicamide; Falcon Pharmaceuticals, Fort Worth, TX). The combination of these two agents did not result in significant elevation of IOP after pharmacologic mydriasis, most likely because of the phenylephrine hypotensive effects, as previously reported in glaucomatous dogs.[27] Corneas were kept moisturized with the use of eye wash solution every 30 to 60 seconds to avoid corneal desiccation. Neuromuscular paralysis was performed to secure eye position in front of the monitor screen (pERG recordings) or within the Ganzfeld dome (full-field ERG recordings). Pattern ERG recordings were performed without prior dark adaptation, whereas scotopic and photopic ERG routines were recorded after 60 minutes of dark adaptation. Contact lens electrodes (ERG Jet electrode; LKC Technologies, Gaithersburg, MD) were used to record ERGs from both eyes. The reference electrode was positioned subcutaneously between the eyes, and the ground electrode was placed subcutaneously in the occipital region of the head.

A Roland Consult (Brandenburg, Germany) ERG system was used to deliver light stimuli and to collect signals from the lens electrode. Standard flash intensity was 2 cd/m^2 = 0 log units. Scotopic ERG responses were measured at −3.5 log units (rod response) and 1.5 log unit (combined rod-cone response) with the following amplification parameters: low-cut amplifier frequency, 1 Hz; high-cut amplifier frequency, 300 Hz. The time interval between stimuli for each light intensity was 14.2 seconds (0.07 Hz), and two responses were averaged per each light intensity. Photopic ERG was recorded using a 0.5 log unit background rod saturating illumination and 1.5 log unit cone flash stimulus (low-cut amplifier frequency, 1 Hz; high-cut amplifier frequency, 300 Hz; time interval between stimuli for each light intensity, 5 seconds [0.2 Hz]; $n = 8$ stimuli were averaged). Oscillatory potentials were recorded using a 1.5 log unit flash stimulus (low-cut amplifier frequency, 200 Hz; high-cut amplifier frequency, 500 Hz; time interval between stimuli for each light intensity, 14.2 seconds [0.07 Hz]; $n = 8$ stimuli were averaged). Photopic flicker was recorded using 0.5 log unit rod saturating illumination and 1.5 log units flickering flash stimulus at a frequency of 20 Hz (low-cut amplifier frequency, 1 Hz; high-cut amplifier frequency, 300 Hz; time interval between each light stimuli was 0.05 seconds [20 Hz]; $n = 50$ stimuli were averaged).

Transient pattern ERG recordings were used to evaluate the retinal ganglion cell function using a 7° checkerboard pattern stimulus with a 2-Hz stimulus frequency, which was projected by a calibrated computer monitor from 20-cm distance from the eyes (low-cut filter, 5 Hz; high-cut filter, 50 Hz; retinal ganglion cell response was evaluated by measuring voltage between the P50 and N95 recording points by averaging 200 signals).

Gonioscopy, Retinoscopy, Cephalic Index Measurement, and High-Frequency Ultrasonography Imaging of the Anterior Segment

High-frequency ultrasonography of the anterior segment was performed using a high-frequency ultrasonography (HFU) unit with the 35-MHz probe (E-Technologies, Bettendorf, IA). Axial eye globe length was measured from ocular ultrasound images obtained by using the 12.5-MHz probe. Gonioscopy examination was carried out by using a gonioscopy lens (Koeppe; Ocular Instruments Inc., Bellevue, WA) and a hand-held slit lamp (SL-15; Kowa Optimed Inc., Torrance, CA). Gonioscopy photography was performed by using a gonioscopy lens (Koeppe; Ocular Instruments Inc.) and a hand-held retinal camera (RetCam; Massie Research Laboratories, Pleasanton, CA). Streak retinoscopy was performed in all dogs (Streak Retinoscope; Welch Allyn Inc., Skaneateles Falls, NY). Cephalic index (CI) measurements were performed by calculating a ratio between the skull width and skull length, as previously reported.[28]

Immunohistochemical and Histology Analysis

Eyes were removed from control and glaucomatous dogs: two glaucomatous eyes were removed from our colony Basset Hounds, and two additional glaucomatous eyes were removed from clinical Basset Hound patients with primary closed-angle glaucoma not related to our

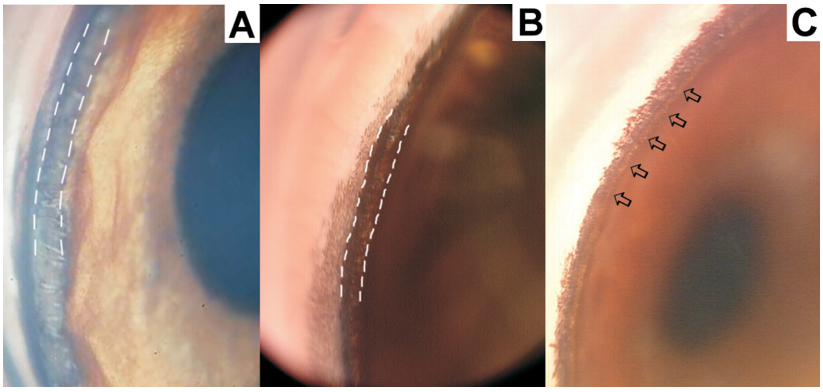

FIGURE 2. (**A**) Gonioscopy photography of a healthy control beagle. *White interrupted lines*: normal width of the iridocorneal angle in healthy dog eye. (**B**) Glaucomatous Basset Hound, age 8 months. *White lines*: decreased width of the iridocorneal angle. (**C**) Glaucomatous Basset Hound, age 20 months. *Arrow*: almost completely collapsed anterior portion of the iridocorneal angle in this dog. This is typical of all glaucomatous dogs from this colony at the age of 20 months.

colony dogs. Eyes were immersion fixed in 4% paraformaldehyde in 0.1 M PO_4 buffer for 1 day and then embedded in paraffin and sectioned at 7 μm. For antibody staining, retinal tissue sections were deparaffinized, washed in phosphate-buffered saline (PBS; 137 mM NaCl, 2.68 mM KCl, 8.1 mM Na_2 HPO_4, 1.47 mM KH_2PO_4), and incubated in blocking solution containing 5% goat serum, 0.4% bovine serum albumin (BSA; Sigma, St. Louis, MO), and 0.2% Triton X-100 (Fisher Scientific, Houston, TX) in PBS. Tissue was incubated overnight at 4°C with an anti-glial fibrillary acidic protein (GFAP, 1:250 dilution; reactive glial cell marker; Dako, Carpinteria, CA) primary antibody diluted in blocking solution. The preparations were then rinsed with PBS and incubated with a secondary antibody (1:1000 dilution; Jackson ImmunoResearch, West Grove, PA) in blocking solution for 90 minutes at room temperature. Sections were washed in PBS and coverslipped (Gelmount mounting media; (Fisher Scientific). Negative controls were carried out in parallel by omission of the primary or secondary antibody. Nonspecific labeling was not observed under these conditions.

Optic nerves were harvested after eye removal and were dissected. Three-millimeter-thick segments obtained 1 mm posterior to the globe were rinsed in cacodylate buffer and postfixed in 2% osmium tetroxide in cacodylate buffer, dehydrated in alcohol, and embedded in epoxy resin. Cross-sections (1-μm thick) were cut with an ultramicrotome, mounted on glass slides, and stained with 1% toluidine blue.

Tissue sections were examined under a photomicroscope (Microphot FXA; Nikon, New York, NY). Images were captured using a camera (Megaplus, model 1.4; Eastman Kodak, Rochester, NY) connected to a frame grabber (MegaGrabber; Perceptics, Knoxville, TN) in a computer (Macintosh 8100/80 AV; Apple Computer, Cupertino, CA) using image acquisition and analysis software (Metamorph; Molecular Devices, Sunnyvale, CA).

Statistical Analysis

Statistical analysis was performed using Student's *t*-test and ANOVA with Bonferroni's posttest with commercial software (Prism, version 5.0; GraphPad, San Diego, CA).

RESULTS

Tonometric Evaluation of IOP

Tonometric evaluation revealed a steady and statistically significant rise in IOP correlated to age in glaucomatous Basset Hounds (Fig. 1). Statistical analysis revealed a significant increase in these values (repeated-measures ANOVA with Bonferroni's multiple comparison posttest, $P = 0.0002$). Intraocular pressure was determined to be 14 ± 0.5 mm Hg (mean ± SEM, 8 months of age), 16 ± 0.85 mm Hg (15 months of age), 17.5 ± 1.2 mm Hg (18 months of age), 25 ± 2.2 mm Hg (20 months of age), and 31.8 ± 5.6 mm Hg (30 months of age). Statistical analysis demonstrates significantly higher IOP values at 20 and 30 months of age compared with values at 8 months (Bonferroni's posttest: $P < 0.01$ IOP_{20m} vs. IOP_{8m}; $P < 0.001$ IOP_{30m} vs. IOP_{8m}), 15 months of age (Bonferroni's posttest: $P < 0.05$ IOP_{20m} vs. IOP_{15m}; $P < 0.01$ IOP_{30m} vs. IOP_{15m}) and 18 months of age (Bonferroni's posttest: $P < 0.01$ IOP_{30m} vs. IOP_{18m}).

Anterior Segment Evaluation

Gonioscopy evaluation showed a gradual narrowing of iridocorneal angles, resulting in complete angle-closure in all evaluated dogs ($n = 6$) by 20 months of age (Fig. 2). HFU demonstrated normal structure of the iridocorneal cleft at 8 months of age but a complete collapse of the iridocorneal cleft by 20 months of age. This collapse was most likely responsible for the gradual increase in intraocular pressure (Fig. 3). Histologic evaluation confirms complete collapse of the ciliary cleft and trabecular meshwork region, consistent with the appearance of angle-closure glaucoma at 20 months of age (Fig. 4).

Evaluation of Refractive Error, Axial Length, and Cephalic Index

Streak retinoscopy evaluation did not reveal a presence of myopia or hyperopia in any evaluated Basset Hounds. Axial eye globe length was calculated in 20-month-old Basset Hounds by performing ocular ultrasound, with values in the range of 20 to 20.8 mm (median, 20.5 mm), which is consistent with previously reported values for healthy dogs.[29] Given that a previous study demonstrated a strong relationship between RGC density and cephalic index,[28] a statistical comparison was performed between cephalic indices for glaucomatous Basset Hounds and healthy beagles. There was no statistical difference between cephalic indices for the sex- and age-matched individuals in two breeds, Beagle CI (81.6 ± 0.9; $n = 6$) and Basset CI (80.3 ± 1.7; $n = 6$) ($P = 0.5$, Student's *t*-test).

Pharmacologic Provocative Testing

Previous studies in human patients with angle-closure glaucoma demonstrated that dark adaptation or pharmacologic pupil dilatation can result in increased IOP in some.[30] We wanted to evaluate whether the pharmacologic use of mydriatic agents can provoke IOP elevation in Basset Hounds with hereditary primary angle-closure glaucoma or in healthy control beagle dogs. An application of a short-acting mydriatic agent (tropicamide) resulted in complete mydriasis and significant elevation of IOP 30 minutes after drug application in Basset Hounds (Fig. 5A; $P < 0.05$, repeated-measures ANOVA with Bonferroni's multiple comparison posttest). Additional application of a long-acting mydriatic agent (atropine 1%) resulted in a further increase in IOP in glaucomatous Basset

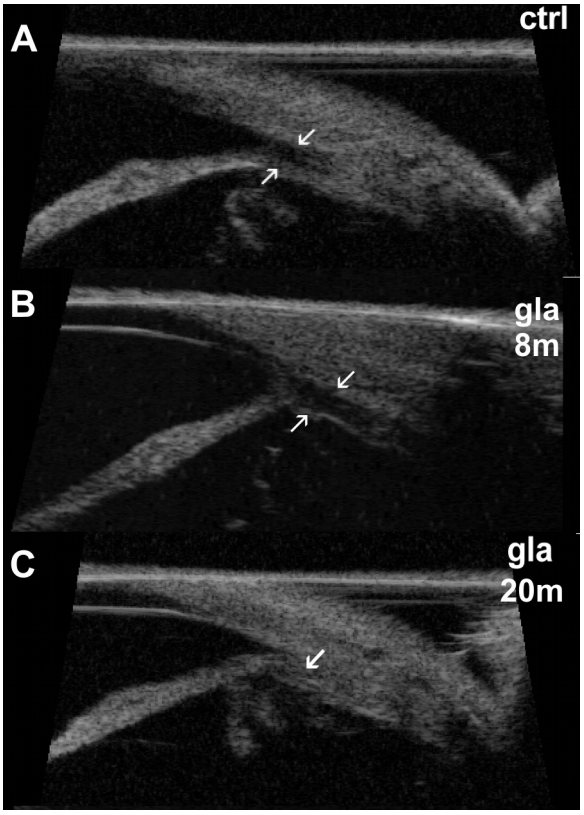

FIGURE 3. High-frequency ultrasound analysis (35-MHz probe) showed a complete collapse of the ciliary cleft and trabecular meshwork in all affected dogs by 20 months of age. (**A**) Image from the healthy control beagle. *Arrows*: normal width of iridocorneal angles. (**B**) Image from a glaucomatous Basset Hound at 8 months of age shows a normal width of the ciliary cleft (*white arrows*). (**C**) Image from a glaucomatous Basset Hound at 20 months of age shows a completely collapsed ciliary cleft (*white arrow*).

Hounds at 18 months of age (Fig. 5A; $P < 0.0001$, repeated-measures ANOVA with Bonferroni's multiple comparison posttest). Application of tropicamide and atropine did not result in the elevation of IOP in control Beagles (Fig. 5A; $n = 10$, $P > 0.1$, repeated measures ANOVA with Bonferroni's multiple comparison test). Administration of a topical prostaglandin F-2α analog (latanoprost 0.005%; Xalatan; Pfizer, New York, NY) and a topical carbonic anhydrase inhibitor (brinzolamide; Azopt 1%; Alcon, Fort Worth, TX) significantly decreased IOP by 69% (Fig. 5A; $P < 0.0001$, repeated-measures ANOVA with Bonferroni's multiple comparison posttest) and 60%, respectively, in Basset Hounds (Fig. 5B; $P < 0.0001$, repeated-measures ANOVA with Bonferroni's multiple comparison posttest).

Electroretinography Analysis

Analysis of the RGC function evaluated by pattern ERG revealed that dogs with glaucoma develop significant and progressive functional deficits as early as 18 months of age (IOP at 18 months of age, 17.5 ± 1.2 mm Hg; glaucomatous = 3.5 ± 0.42 μV; control = 6.2 ± 0.35 μV; $P = 0.004$, Student's *t*-test; Fig. 6A). Pattern ERG amplitudes continued to decline and remained significantly lower in glaucomatous dogs compared with healthy control eyes at 20 months (glaucomatous = 3.3 ± 0.17 μV; control = 6.2 ± 0.35 μV; $P < 0.0001$, Student's *t*-test; Fig. 6A) and 30 months of age (glaucomatous = 1.84 ± 1 μV; control = 6.2 ± 0.35 μV; $P = 0.0002$, Student's *t*-test; Fig. 6A).

Linear regression analysis indicates a significant correlation between pERG amplitudes and IOP levels at the time of recording ($P < 0.0001$; $r^2 = 0.87$).

Given that affected Basset Hounds display pERG deficits even at 18 months of age (Fig. 6), before marked increases in IOP (14 vs. 17.5 mm Hg), we wanted to evaluate whether diurnal IOP variation could be responsible for the observed functional deficits. Diurnal IOP recordings revealed IOP increases during the dark period (17.6 ± 2.6 mm Hg, day; 22.2 ± 1.9 mm Hg, night). However, this difference was not statistically significant ($P = 0.07$, paired *t*-test). The development of pERG deficits before the development of high IOP does not occur only in our Basset Hound colony. We further evaluated the eyes of three canine primary glaucoma patients of different breeds (two Siberian Husky dogs and one Shetland Sheepdog), which developed aggressive elevation of IOP in one eye, whereas the opposite eye had collapsed iridocorneal angles but normal IOP and no clinical or historical evidence of ocular problems (Fig. 7). These fellow eyes were considered nonaffected by acute glaucoma at the time of evaluation and did not receive medical or surgical treatment. However, clinical experience in canine ophthalmology indicates that the fellow eyes are not normal and likely will develop glaucoma within the next 6 to 12 months.

Pattern ERG, scotopic and photopic ERG routines, and IOPs were recorded from these nonaffected eyes and compared with values obtained from glaucomatous Bassets at 18 months of age and healthy Beagle dogs (Fig. 7). Pattern ERG recordings revealed dramatically decreased amplitudes in the nonaffected eyes of all dogs with primary glaucoma despite normal IOPs at the time of clinical evaluation. These findings suggest that

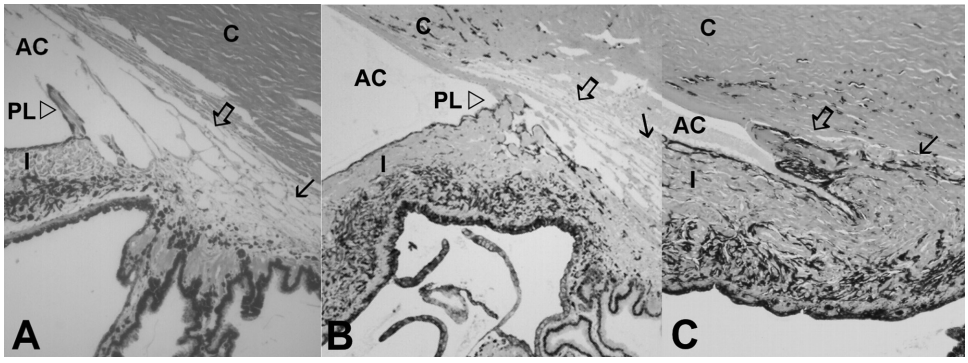

FIGURE 4. (**A**) Histologic appearance of the anterior segment in healthy control eye. *Open arrow*: ciliary cleft. *Closed arrow*: trabecular meshwork region. *Closed arrowhead*: pectinate ligament. (**B**) Histologic appearance of one of our colony dogs at 8 months of age. The ciliary cleft (*open arrow*) is open, and the trabecular meshwork region is wide and well organized, as in the control dog (*closed arrow*). Pectinate ligament (PL, *open arrowhead*) has some narrow appearance compared to the healthy control dog. (**C**) Histologic appearance of one of our colony dogs at 20 months of age. The ciliary cleft (*open arrow*) is completely collapsed, and the trabecular meshwork region is almost completely compressed by the base of the iris (*closed arrow*). AC, anterior chamber; C, cornea; I, iris; PL, pectinate ligament.

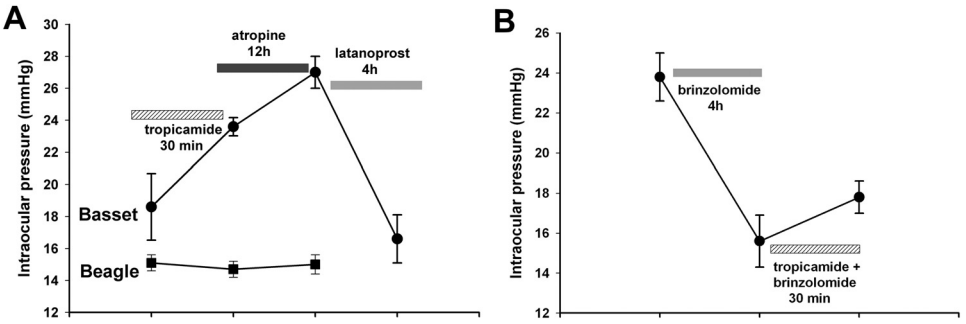

FIGURE 5. (**A**) Mydriatic agents (tropicamide and atropine 1%) provoke significant elevation of IOPs in glaucomatous dogs by 35% and 50%, respectively, above the baseline values (18 month old dogs; $n = 6$). Latanoprost effectively reduces IOPs below the baseline levels within 4 hours of application. Provocative testing in control Beagle dogs did not cause any elevation of IOP. Values are presented as mean ± SEM. (**B**) Carbonic anhydrase inhibitor (brinzolomide) induced significant reduction of IOPs in glaucomatous eyes (testing was performed at 20 months of age; $n = 6$). Subsequent application of mydriatic agent slightly elevated IOP (change was not statistically significant; $n = 6$; $P > 0.1$, repeated-measures ANOVA with Bonferroni's multiple comparison posttest); however, the range remained close to 18 mm Hg.

functional deficits may precede significant elevation of IOP in many cases of canine glaucoma, as we demonstrated in our colony dogs (Figs. 6–8).

Because of the significant decrease in pERG amplitudes at relatively normal IOP levels, we performed a detailed analysis of scotopic and photopic ERG function to determine whether possible abnormalities in the outer retina could be responsible for observed pERG deficits (Fig. 9). Scotopic ERG analysis of glaucomatous dogs did not reveal significant functional deficits for the rod-mediated b-wave amplitudes ($P = 0.84$, Student's *t*-test), rod-cone mediated a-wave amplitudes ($P = 0.97$, Student's *t*-test), and rod-cone b-wave amplitudes ($P = 0.97$, Student's *t*-test) compared with healthy control beagle eyes. Statistical analysis of oscillatory potential components did not reveal significant differences for OP1 ($P = 0.94$, Student's *t*-test), OP2 ($P = 0.08$), OP3 ($P = 0.84$), or OP4 ($P = 0.18$) amplitudes (Fig. 9) between 20-month-old Basset Hounds and healthy control beagles. Statistical analysis of cone-mediated responses also did not show significant differences between 20-month-old Bassets and healthy control beagles for photopic a-wave ($P = 0.09$, Student's *t*-test), photopic b-wave ($P = 0.25$), and photopic flicker ($P = 0.33$) amplitudes.

Histologic Analysis

Histologic analysis of glaucomatous eyes revealed collapse of the iridocorneal angles and trabecular meshwork (Fig. 4) and deformation of the lamina cribrosa region (bowing of the lamina cribrosa) with early development of optic nerve head cupping (Fig. 10B). Immunohistochemical analysis for glial reactive changes, as indicated by GFAP expression, in our dogs showed mild glial reactivity at the optic nerve head region and minimal glial reactivity at the peripapillary nerve fiber layer compared with clinical patients with more advanced stages of disease (Fig. 10). Histologic sections of the retina from our colony dogs revealed normal retinal architecture with primary loss of large RGCs and mild glial reactive changes that could be detected in the nerve fiber layer compared with healthy control eyes (Fig. 11). Cross-section of the optic nerve revealed predominant degeneration of large axons, extensive glial proliferation/hypertrophy, and possible increase in the intercellular matrix deposits (Fig. 12).

DISCUSSION

The experimental approach used in this study allowed us to determine the dynamics of functional, structural and IOP changes in dogs with a hereditary form of PACG over 30 months. The anatomy of the canine anterior segment has significant differences compared with the human eye that must be taken in account when evaluating the results of this study. Canine eyes have pillars of tissue (pectinate ligaments) as the most anterior part of the iridocorneal angle, which are projecting from the base of iris to the peripheral Descemet's membrane. It has been speculated that pectinate ligaments may be structurally similar to iris processes in human eyes.[31] Posterior to the pectinate ligament is a wide region of the ciliary cleft that continues in the uveal and corneoscleral trabecular meshwork. A classic study by Morrison and Van Buskirk[31] demonstrated that the pectinate ligament and the width of the ciliary cleft have a significant effect on the aqueous humor outflow in canine eyes.

We demonstrated that in this particular model the iridocorneal angles and trabecular meshwork structures collapse, which was evident during serial gonioscopy and, high-frequency ultrasound examinations and was ultimately confirmed

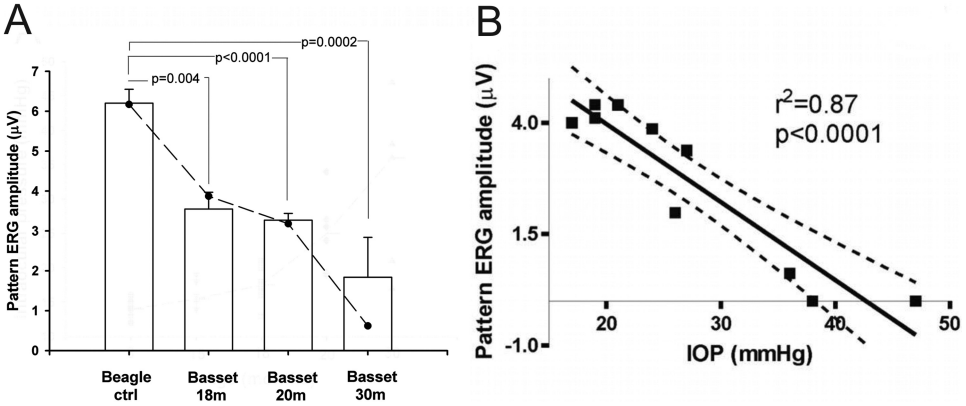

FIGURE 6. (**A**) Pattern ERG recordings reveal progressive development of electrophysiological deficits in Basset Hounds with primary angle-closure glaucoma (P50-N95 amplitudes were calculated). *Dashed line* connects median values for each group. Bars represent mean + SEM values. (**B**) Linear regression analysis shows good correlation between IOP and pERG amplitudes. *Dashed lines*: 95% confidence interval.

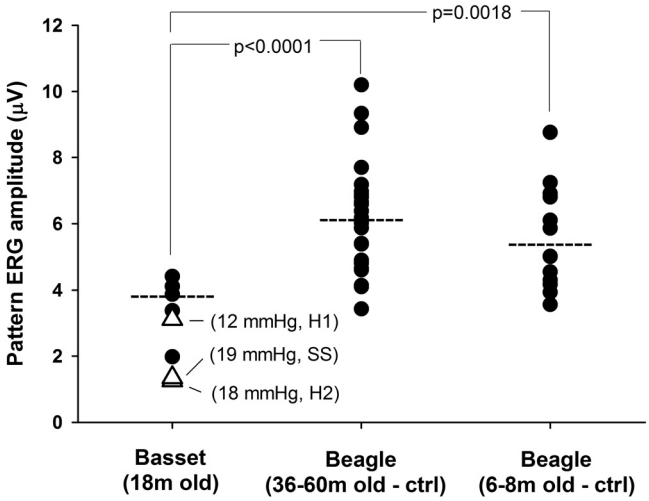

FIGURE 7. (**A**) Pattern ERG amplitudes (P50-N95 values) are significantly decreased in 18-month-old Basset Hounds with slightly elevated IOP (*circles*) and in the normotensive fellow eyes of two other breeds of dogs affected with primary glaucoma (*triangles*) compared with young and adult healthy Beagles (H1, Siberian Husky, male, 3 years old; H2, Siberian Husky, female, 5 years old; SS, Shetland Sheepdog, male, 5 years old). There was no statistical difference between young and old Beagle pERG amplitudes ($P = 0.7$, Student's *t*-test).

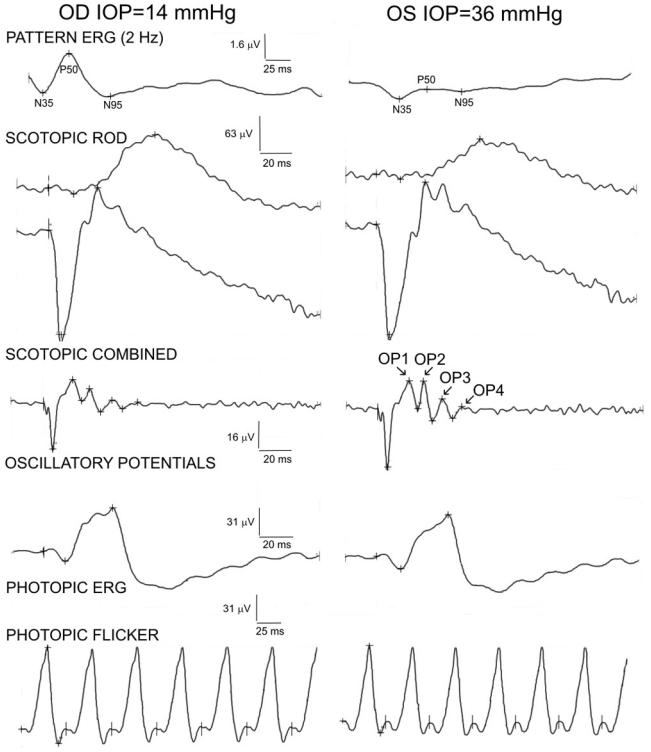

FIGURE 9. Detailed ERG analysis revealed the presence of dramatic retinal ganglion cell dysfunction in glaucomatous Basset Hound eyes observed by pERG recordings (steady state pERG 2Hz frequency with 7° grating stimulus). *Arrow*: pERG tracing from a glaucomatous canine patient with an IOP of 36 mm Hg. RGC function was evaluated by measuring P50-N95 interval, which was almost completely extinguished in this eye. The rest of the routines did not show functional deficits in other retinal neuronal populations: scotopic rod response evaluates rod function; scotopic combined response evaluates function of rods and cones (with associated inner nuclear layer neurons and Müller cells); oscillatory potentials evaluate the function of amacrine cells and synaptic connections in the inner plexiform layer; photopic ERG response evaluates the function of cones and associated inner retinal neurons, and photopic flicker evaluates the function of inner retinal neurons (bipolar cells) mediating cone signal transduction. The recordings were obtained from the 30-month-old Basset Hound from the right and left eye, respectively.

by histologic analysis. These structural changes are the most likely cause for the observed gradual increase in IOP.

Previous studies have demonstrated acute elevation of IOP in patients with PACG after use of topical mydriatic agents.[32,33] Our data showed that consistent and significant acute elevation of IOP after treatment with topical mydriatic agents also occurs in our dogs, further confirming similarities observed between animals and at least some human patients with PACG. Analogous to previously published data from human patients with PACG, we demonstrate herein that prostaglandin analogs and carbonic anhydrase inhibitors have a potent effect on lowering IOP in Basset Hounds with PACG, further confirming the value of this model for the potential development of new IOP-lowering drugs.[33,34]

Our data demonstrated the development of significant and progressive RGC functional deficits during the course of disease, which correlates well with the increase in IOP as previously reported in humans and mice with glaucoma.[21,35–37]

We hypothesize that, over time, abnormal structural support leads to the gradual collapse of the iridocorneal angles and the lamina cribrosa, which may explain the observed functional deficits at 18 months of age despite relatively normal intraocular pressure. However, we cannot completely exclude the possibility that intermittent IOP spikes may be responsible for the observed early functional deficits in Basset Hounds. With the progression of the anterior segment structural changes, IOP continues to increase and likely has additional

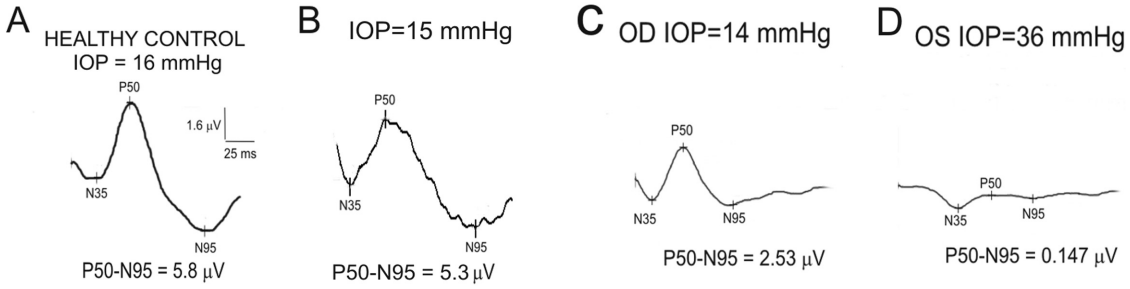

FIGURE 8. Pattern ERG tracings showed minimal reduction in a young (7 months, F2 generation), sex-matched Basset Hound from our colony (**B**) compared with healthy control Beagle eyes (**A**). Pattern ERG analysis showed a dramatic reduction in the P50-N95 amplitudes in normotensive (**C**) and hypertensive (**D**) adult Basset Hound glaucoma eyes (F1 generation; C, recording at 18 months of age; D, opposite eye of the same animal during provocative ocular hypertension after topical atropine 1% administration at 18 months of age).

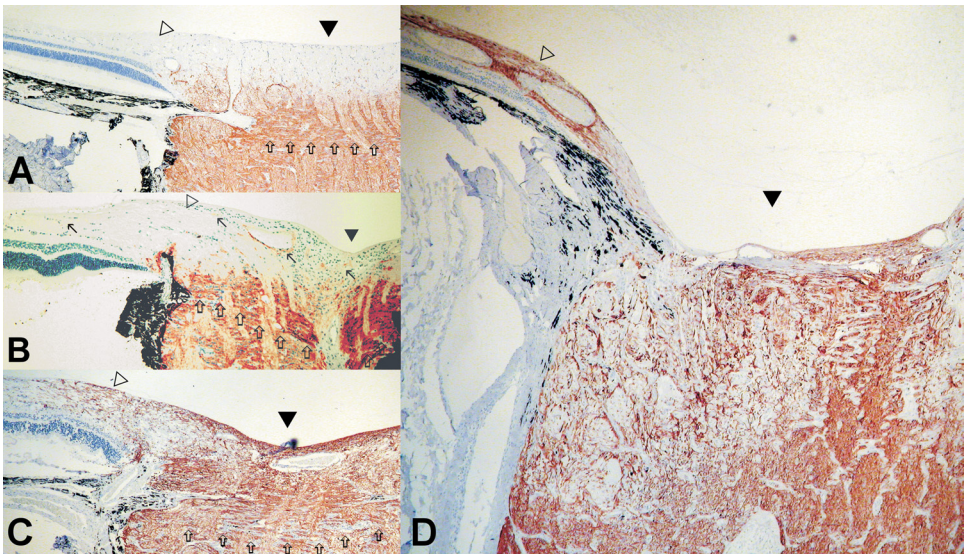

FIGURE 10. (**A**) Histologic appearance of a healthy control optic nerve head (ONH), and peripapillary ONH region shows a flat surface of the ONH (*black arrowhead*), lack of GFAP immunoreactivity (*red*) in the nerve fiber layer (*white arrowhead*), and horizontal organization of the lamina cribrosa (*open arrows*). (**B**) Histology section from one of our colony dogs (20 months old; IOP was 24 mm Hg at the time of eye removal). *Black arrowhead*: early formation of the ONH cup. *White arrowhead*: thickened peripapillary nerve fiber layer with minimal presence of reactive glial changes (*black arrows*). *Open arrows*: posterior bowing of the lamina cribrosa region. (**C**) Glaucomatous eye from a 5-year-old Basset Hound with primary glaucoma. The disease was medically treated for 3 months before eye removal; IOP at the time of eye removal was 32 mm Hg. Histologic changes are similar to changes observed in (**B**), but more extensive cupping and glial reactive changes (*red*) are present. (**D**) Glaucomatous eye from a 6-year-old Basset Hound with primary glaucoma. The disease was medically treated for 8 months before eye removal because of complete blindness and poor intraocular pressure control (IOP at the time of eye removal was 38 mm Hg). This patient has severe cupping and deformation of the ONH region. Severe glial reactive changes are present in the peripapillary nerve fiber layer (*white arrowhead* points to intensive red staining of the NFL).

detrimental effects on the optic nerve head structure and vascular supply of the optic nerve head.[38–41] Our data also demonstrate the presence of prominent pattern ERG deficits despite apparently normal IOP, which occurs in other canine breeds affected with primary glaucoma as well. Taken together, these findings support the hypothesis that pERG functional deficits are an early indicator of disease progression in canine glaucoma. Although there is a possibility that our control population (healthy beagles) may have higher physiological pERG amplitudes, this is considered unlikely because the number and retinal topographic distribution of RGCs does not differ significantly between the breeds of dogs used in this study.[28] Considering that CI value can have a significant impact on RGC density (which could influence pattern ERG amplitudes), we performed a calculation of CIs for both breeds (healthy Beagles and glaucomatous Bassets) and did not detect a statistically significant difference. This observation further supports our hypothesis that observed functional deficits in glaucomatous Basset Hounds, before significant and sustained elevation of IOP development, are indeed the result of a pathologic process rather than a physiological difference in RGC distribution between two breeds.

The ideal control population for this study would be healthy, age-matched Basset Hounds; however, considering the relatively high incidence of glaucoma in this particular breed and a possibility that many apparently healthy dogs are subclinically affected, we decided to use experimental healthy beagles with a glaucoma-free pedigree as a more reliable control population. All breeds and dogs assessed in this study (with the exception of healthy laboratory Beagles) were from our glaucomatous colony or from clinical canine glaucoma patients treated at our hospital, so it is highly unlikely that in this dog

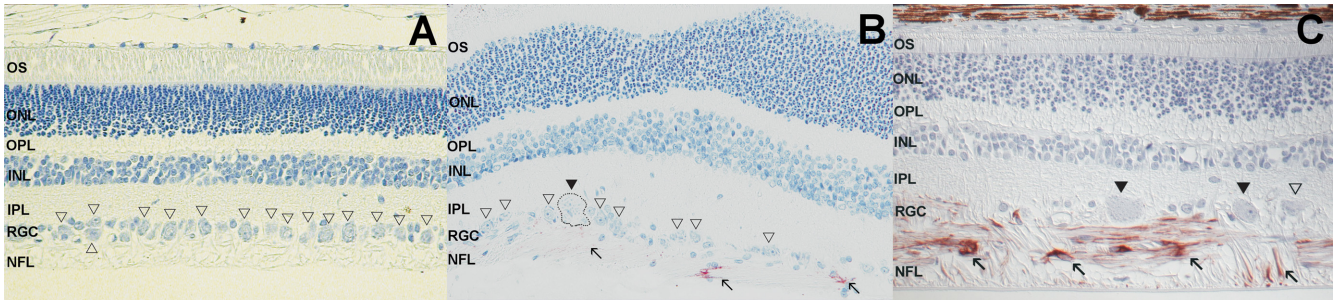

FIGURE 11. Loss of large retinal ganglion cells is the primary feature of canine hereditary glaucoma. (**A**) Control healthy retina. GFAP staining (large RGC count reveals 12 to 15 cells per optic field). *Open arrowheads*: large RGCs. (**B**) Glaucomatous retina from a colony Basset Hound (Fig. 10B shows ONH histology from the same dog). Retinal architecture is still well preserved, but the number of large RGCs is decreased (8 cells per optic field; *open arrowheads*). *Dark arrowhead*: large swollen RGCs seen in this histology section; cell membrane was delineated with *dark color* to demonstrate 100% to 200% increase in size of the cell body compared with neighboring large RGCs. Mild glial reactivity can be detected in the NFL (*arrows* point *red*-stained regions in the NFL). (**C**) Basset Hound with advanced primary glaucoma (histology retinal section corresponds to the dog shown in Fig. 10D). Severe reactive glial changes are present in the NFL (*black arrows* point to the *red*-GFAP staining, and *white arrowheads* point to one large retinal ganglion cell. *Dark arrowheads*: two large swollen retinal ganglion cells. This retinal section shows pan-retinal degenerative changes with the neuronal loss in the inner and outer nuclear layers and shortening of the photoreceptor outer segments. NFL, nerve fiber layer; RGC, retinal ganglion cells; IPL, inner plexiform layer; INL, inner nuclear layer; OPL, outer plexiform layer; ONL, outer nuclear layer; OS, outer segments.

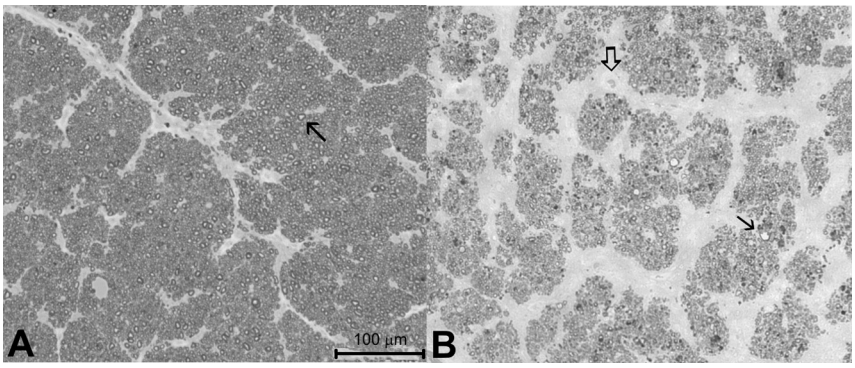

FIGURE 12. (**A**) Cross-section histology of the healthy (control) canine optic nerve 1 mm posterior to the laminar region. *Arrow*: large axonal profile in the healthy optic nerve. (**B**) Cross-section histology of the optic nerve 1 mm posterior to the laminar region from one colony of glaucomatous Basset Hounds (30 months of age; IOP at the time of eye removal was 36 mm Hg). Massive degeneration of predominantly large axons is evident. Some axons are extremely swollen and enlarged (*closed arrow*). Excessive glial proliferation/hypertrophy (*open arrow*) and thickening of septa can be observed between axon bundles and within axon bundles in this section. Observed axonal loss was of rather diffuse nature, and images of both eyes were collected from the superior central portion of the optic nerve, where thickening of the laminar septa appeared most prominent.

population decreased pERG amplitudes were the result of physiological variation rather than the disease process. In support of our data, we show the pERG tracing from a young colony Basset Hound at the age of 7 months (Fig. 8B) indicating near normal values compared with the age-matched healthy control Beagles. Our major justification for not using adult healthy Basset Hounds as a control is the fact that almost 70% of healthy Basset Hounds have some degree of the pectinate ligament and ciliary cleft abnormalities seen in glaucomatous dogs of different breeds (SDG, unpublished observation, 2009). Considering that similar abnormalities may persist at the level of the optic nerve head, we were concerned that pERG recording in Basset Hounds that were nonglaucomatous and used as a control population would not provide optimal control data because of the relatively high possibility that some of examined dogs could be mutation carriers or even undiagnosed glaucoma-affected dogs. Because elevation of intraocular pressure and acute signs of angle-closure glaucoma in Basset Hounds can develop even in 8- to 10-year-old animals, we cannot be certain about the glaucoma status in any control Basset Hound until a reliable genetic test is developed.

Furthermore, we recently demonstrated that early pERG deficits in glaucomatous Basset Hounds can be significantly reversed with the use of the topical indirect cholinergic drug demecarium bromide (Grozdanic SD, et al. *IOVS* 2009;50: ARVO E-Abstract 2784; manuscript in preparation), which further supports our notion that observed pERG deficits are indeed the result of a disease process rather than a physiological difference between breeds of dogs.

Histologic observation of retinas and optic nerves in glaucomatous Basset Hounds revealed early posterior bowing of the lamina cribrosa, loss of large optic nerve axons (and also swelling and loss of large retinal ganglion cells), and predominant central thickening of the optic nerve septae. Similar morphologic observations have been reported in a model of canine hereditary glaucoma in Beagles in which Brooks et al.[42] demonstrated predominant loss of large axons, especially in the central optic nerve regions. Yang et al.[43] demonstrated that the earliest changes in monkey eyes with laser-induced ocular hypertension are laminar deformation and thickening with posterior bowing and prelaminar neural tissue thickening, which in many aspects corresponds to the histologic changes observed in glaucomatous Basset Hounds. A recent elegant study by Roberts et al.[44] explored in great detail the connective tissue architecture of the lamina cribrosa in monkeys with early-stage ocular hypertension. This particular study provided very strong evidence of early optic nerve susceptibility to an increase in laminar connective tissue in central and superior optic nerve regions that offers a possible explanation for laminar changes and preferential central axonal loss in dogs with hereditary forms of glaucoma, as previously reported[42] and also described in this study.

The Basset Hound PACG model offers a unique opportunity for more detailed structural, functional, and molecular studies in early glaucoma. The availability of canine genome data and microarray resources for analysis provide excellent tools to study the complex genetic changes in the optic nerve and retina of glaucoma in affected animals (Jiang B, et al. *IOVS* 2007;48:ARVO E-Abstract 5901).

The hereditary model of Basset Hound PACG shares many features of PACG in humans and may hold great potential for better understanding of glaucomatous optic nerve damage. Given that glaucoma in our colony affected 100% of all dogs, we speculate that the PACG in Basset Hounds is the most likely a result of a hereditary genetic defects in one (or more) genes, possibly involved in the synthesis/regulation of structural molecules at the level of anterior segment (iridocorneal angle) and maybe the laminar region of the optic nerve head. Possible future identification of the gene (or genes) responsible for the observed functional and structural changes in this form of hereditary glaucoma may dramatically increase our understanding of physiological and disease-changed optic nerve properties in humans and animals.

References

1. Quigley HA. Neuronal death in glaucoma. *Prog Retin Eye Res.* 1999;18(1):39–57.
2. Morrison JC. Elevated intraocular pressure and optic nerve injury models in the rat. *J Glaucoma.* 2005;14(4):315–317.
3. Levin LA. Direct and indirect approaches to neuroprotective therapy of glaucomatous optic neuropathy. *Surv Ophthalmol.* 1999; 43(suppl 1):S98–S101.
4. Osborne NN, Chidlow G, Nash MS, Wood JP. The potential of neuroprotection in glaucoma treatment. *Curr Opin Ophthalmol.* 1999;10(2):82–92.

5. Boland MV, Quigley HA. Risk factors and open-angle glaucoma: classification and application. *J Glaucoma.* 2007;16(4):406–418.
6. Hayreh SS. The role of age and cardiovascular disease in glaucomatous optic neuropathy. *Surv Ophthalmol.* 1999;43(suppl 1): S27–S42.
7. Rasmussen CA, Kaufman PL. Primate glaucoma models. *J Glaucoma.* 2005;14(4):311–314.
8. Levkovitch-Verbin H. Animal models of optic nerve diseases. *Eye.* 2004;18(11):1066–1074.
9. Quigley HA, Addicks EM. Chronic experimental glaucoma in primates, I: production of elevated intraocular pressure by anterior chamber injection of autologous ghost red blood cells. *Invest Ophthalmol Vis Sci.* 1980;19(2):126–136.
10. Quigley HA, Addicks EM. Chronic experimental glaucoma in primates, II: effect of extended intraocular pressure elevation on optic nerve head and axonal transport. *Invest Ophthalmol Vis Sci.* 1980;19(2):137–152.
11. Jonas JB, Hayreh SS. Influence of experimental chronic high-pressure glaucoma on age-related macular degeneration in rhesus monkeys. *Invest Ophthalmol Vis Sci.* 2000;41(10):2972–2977.
12. Garcia-Valenzuela E, Shareef S, Walsh J, Sharma SC. Programmed cell death of retinal ganglion cells during experimental glaucoma. *Exp Eye Res.* 1995;61(1):33–44.
13. Morrison JC, Moore CG, Deppmeier LM, et al. A rat model of chronic pressure-induced optic nerve damage. *Exp Eye Res.* 1997; 64(1):85–96.
14. Levkovitch-Verbin H, Quigley HA, Martin KR, et al. Translimbal laser photocoagulation to the trabecular meshwork as a model of glaucoma in rats. *Invest Ophthalmol Vis Sci.* 2002;43(2):402–410.
15. Grozdanic SD, Kwon YH, Sakaguchi DS, et al. Functional evaluation of retina and optic nerve in the rat model of chronic ocular hypertension. *Exp Eye Res.* 2004;79(1):75–83.
16. Grozdanic SD, Betts DM, Sakaguchi DS, et al. Temporary elevation of the intraocular pressure by cauterization of vortex and episcleral veins in rats causes functional deficits in the retina and optic nerve. *Exp Eye Res.* 2003;77(1):27–33.
17. Grozdanic SD, Betts DM, Sakaguchi DS, et al. Laser-induced mouse model of chronic ocular hypertension. *Invest Ophthalmol Vis Sci.* 2003;44(10):4337–4346.
18. John SW, Smith RS, Savinova OV, et al. Essential iris atrophy, pigment dispersion, and glaucoma in DBA/2J mice. *Invest Ophthalmol Vis Sci.* 1998;39(6):951–962.
19. Scholz M, Buder T, Seeber S, et al. Dependency of intraocular pressure elevation and glaucomatous changes in DBA/2J and DBA/2J-Rj mice. *Invest Ophthalmol Vis Sci.* 2008;49(2):613–621.
20. McKinnon SJ, Schlamp CL, Nickells RW. Mouse models of retinal ganglion cell death and glaucoma. *Exp Eye Res.* 2009;88:816–824.
21. Nagaraju M, Saleh M, Porciatti V. IOP-dependent retinal ganglion cell dysfunction in glaucomatous DBA/2J mice. *Invest Ophthalmol Vis Sci.* 2007;48(10):4573–4579.
22. Porciatti V, Saleh M, Nagaraju M. The pattern electroretinogram as a tool to monitor progressive retinal ganglion cell dysfunction in the DBA/2J mouse model of glaucoma. *Invest Ophthalmol Vis Sci.* 2007;48(2):745–751.
23. Saleh M, Nagaraju M, Porciatti V. Longitudinal evaluation of retinal ganglion cell function and IOP in the DBA/2J mouse model of glaucoma. *Invest Ophthalmol Vis Sci.* 2007;48(10):4564–4572.
24. Howell GR, Libby RT, Jakobs TC, et al. Axons of retinal ganglion cells are insulted in the optic nerve early in DBA/2J glaucoma. *J Cell Biol.* 2007;179(7):1523–1537.
25. Gelatt KN, Brooks DE, Samuelson DA. Comparative glaucomatology, I: the spontaneous glaucomas. *J Glaucoma.* 1998;7(3):187–201.
26. Gelatt KN, Peiffer RL Jr, Gwin RM, et al. Clinical manifestations of inherited glaucoma in the beagle. *Invest Ophthalmol Vis Sci.* 1977;16(12):1135–1142.
27. Gwin RM, Gelatt KN, Gum GG, Peiffer RL Jr. Effects of topical 1-epinephrine and dipivalyl epinephrine on intraocular pressure and pupil size in the normotensive and glaucomatous Beagle. *Am J Vet Res.* 1978;39(1):83–86.
28. McGreevy P, Grassi TD, Harman AM. A strong correlation exists between the distribution of retinal ganglion cells and nose length in the dog. *Brain Behav Evol.* 2004;63(1):13–22.
29. Murphy CJ, Zadnik K, Mannis MJ. Myopia and refractive error in dogs. *Invest Ophthalmol Vis Sci.* 1992;33(8):2459–2463.
30. Mapstone R. Dilating dangerous pupils. *Br J Ophthalmol.* 1977; 61(8):517–524.
31. Morrison JC, Van Buskirk EM. The canine eye: pectinate ligaments and aqueous outflow resistance. *Invest Ophthalmol Vis Sci.* 1982; 23(6):726–732.
32. Mapstone R. Closed-angle glaucoma: experimental results. *Br J Ophthalmol.* 1974;58(1):41–45.
33. Edwards RS. Behaviour of the fellow eye in acute angle-closure glaucoma. *Br J Ophthalmol.* 1982;66(9):576–579.
34. Chen MJ, Chen YC, Chou CK, Hsu WM. Comparison of the effects of latanoprost and travoprost on intraocular pressure in chronic angle-closure glaucoma. *J Ocul Pharmacol Ther.* 2006;22(6):449–454.
35. Bach M, Unsoeld AS, Philippin H, et al. Pattern ERG as an early glaucoma indicator in ocular hypertension: a long-term, prospective study. *Invest Ophthalmol Vis Sci.* 2006;47(11):4881–4887.
36. Parisi V, Miglior S, Manni G, et al. Clinical ability of pattern electroretinograms and visual evoked potentials in detecting visual dysfunction in ocular hypertension and glaucoma. *Ophthalmology.* 2006;113(2):216–228.
37. Ventura LM, Porciatti V. Restoration of retinal ganglion cell function in early glaucoma after intraocular pressure reduction: a pilot study. *Ophthalmology.* 2005;112(1):20–27.
38. Burgoyne CF, Quigley HA, Thompson HW, et al. Early changes in optic disc compliance and surface position in experimental glaucoma. *Ophthalmology.* 1995;102(12):1800–1809.
39. Yang H, Downs JC, Girkin C, et al. 3-D histomorphometry of the normal and early glaucomatous monkey optic nerve head: lamina cribrosa and peripapillary scleral position and thickness. *Invest Ophthalmol Vis Sci.* 2007;48(10):4597–4607.
40. Burgoyne CF, Downs JC, Bellezza AJ, Hart RT. Three-dimensional reconstruction of normal and early glaucoma monkey optic nerve head connective tissues. *Invest Ophthalmol Vis Sci.* 2004;45(12): 4388–4399.
41. Sihota R, Saxena R, Taneja N, et al. Topography and fluorescein angiography of the optic nerve head in primary open-angle and chronic primary angle-closure glaucoma. *Optom Vis Sci.* 2006; 83(7):520–526.
42. Brooks DE, Strubbe DT, Kubilis PS, et al. Histomorphometry of the optic nerves of normal dogs and dogs with hereditary glaucoma. *Exp Eye Res.* 1995;60(1):71–89.
43. Yang H, Downs JC, Burgoyne CF. Physiologic intereye differences in monkey optic nerve head architecture and their relation to changes in early experimental glaucoma. *Invest Ophthalmol Vis Sci.* 2009;50(1):224–234.
44. Roberts MD, Grau V, Grimm J, et al. Remodeling of the connective tissue microarchitecture of the lamina cribrosa in early experimental glaucoma. *Invest Ophthalmol Vis Sci.* 2009;50(2):681–690.